

Structural optimization of an automotive wheel rim through an RBF mesh morphing technique

Emiliano Costa

D'Appolonia SpA

Rome, Italy

Web: <http://www.dappolonia.it>

Corrado Groth, Marco E. Biancolini, Francesco Giorgetti, Andrea Chiappa

University of Rome Tor Vergata

Rome, Italy

Web: <http://dii.uniroma2.it>

Corresponding Author: emiliano.costa@dappolonia.it

Summary

In this paper a novel approach to handle the structural design and automate the shape optimization of an automotive wheel rim in the ANSYS Workbench environment is proposed. The aim of the study is to optimize an aluminium wheel rim taking into account the testing conditions dictated by a protocol conceived to get the approval for the certification of such a mechanical component.

Using the baseline CAD of the model, the modifications to be computationally investigated for optimization purposes have been applied through a mesh morphing technique using RBF Morph ACT Extension.

Specifically, after the judgment of the numerical outputs obtained under the prescribed loading and constraint scenarios considered for the baseline FEM model, the RBF solutions driving the moulding of the component have been set to identify the optimal configuration representing the best trade-off between maximum stress present in the component, its mass as well as its structural behaviour in terms of inertial characteristics. A mass reduction of about 7% is achieved satisfying all the strength requirements imposed by the protocol.

Keywords

Optimization, mesh morphing, radial basis functions, meshless, ANSYS Workbench, ANSYS Mechanical.

Introduction

Structural optimization is a method commonly employed by designers to realize better products as soon as possible. In the present work the aim is to arrange the material distribution of a structure in order to get the minimum weight and to prevent the risk of mechanical failure during its functioning. There are several ways to accomplish the structural optimization task. Topology optimization allows to reduce the mass of a component subjected to specific loads and constraints, by removing material from a defined design space [1]. Given that, although the location of mesh nodes is maintained fixed, the structural behaviour of the component changes during the optimization cycles because of material removal. Shape optimization is somehow complementary to topology optimization: the material distribution of full and empty parts of a structure is preserved but mesh nodes location, and consequently the volume of elements, are changed to get the optimal configuration typically identifying the suitable trade-off between strength and weight [2]. Considering the characteristics of both, topology and shape optimizations can be performed in sequence because, once the topology is specified, the shape optimization can be accordingly accomplished. An effective way to handle the latter stage is to use CAD-based optimizations founded on the geometrical parameterization of the shape of constituting components. The workflow of these methods is qualitatively depicted in Figure 1a. Although this kind of approach is almost the standard practice for designers to optimize the geometry in an automatic manner [3], it is, however, affected by a series of limitations such as the need for preserving the coherence during optimization, the re-meshing noise due to CAD reconstruction that affects FEA results and the fact that not all geometrical features can be efficiently parameterized. Mesh morphing-based techniques are an alternative method to carry out shape optimizations avoiding the aforementioned limitations. It is well known that such a method is used for shape optimization when parametric geometries are too complex to be properly managed by means of CAD-based strategies [4]-[5]. An interesting study about volume mesh morphing using Radial Basis Functions (RBF) is presented in [6], where both linear and cubic functions are used for the updating

of a volume mesh using CAD controlled points at surfaces. RBF are the mathematical foundation of the commercial morphing software RBF Morph™, are well recognized [7] to enjoy, to name few, the high local control of mesh nodes and flexibility that comes with many advantages associated with their meshless nature. The workflow of mesh morphing-based shape optimizations is qualitatively shown in Figure 1b.

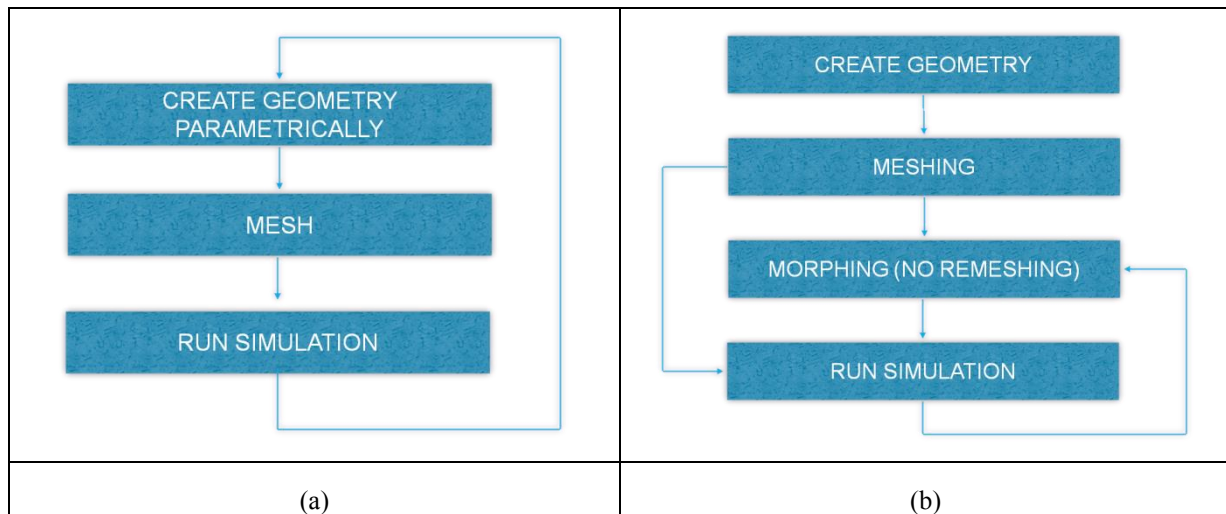


Figure 1: CAD-based versus mesh morphing-based optimization workflow

By means of the ANSYS ACT technology, a brand new implementation of the acclaimed and well-established RBF Morph software, is now available for ANSYS® Mechanical™. Through this tool the optimization of an automotive wheel rim aiming at achieving light weight and structural consistency has been accomplished. This optimization analysis is part of a set of explorative studies performed in the frame of the technical collaboration between D’Appolonia (RINA Group) and the University of Rome “Tor Vergata” supported by RBF Morph, having the purpose to evaluate the capabilities of RBF mesh morphing-based procedures for design and optimization in the industrial sector as well as to quantify the time they permit to save with respect to the currently adopted methodologies.

Background on RBF mesh morphing

A system of RBFs is used to produce a solution for mesh morphing, once a list of source points and their displacements is defined. This approach is valid both for surfaces shape changes and volume mesh smoothing. RBFs are a very powerful tool created for the interpolation of scattered data [8]. As a matter of fact, they are able to interpolate everywhere within the space a function that is defined at discrete points giving the exact value at original points. The interpolation quality, as well as its behaviour between points, depends on the kind of adopted basis.

RBFs can be classified on the basis of the type of support (global or compact) they have, meaning the domain where the chosen RBF is non zero-valued [9]. Typical RBF functions are shown in Table 1. RBFs are scalar functions with the scalar variable r which, in the case of mesh morphing, can be assumed to be the Euclidean norm of the distance between two points defined in a three-dimensional space. In some cases, a polynomial corrector is added to guarantee the existence of an RBF fit.

RBF with global support	$\varphi(r)$
Spline type (Rn)	$r^n, n \text{ odd}$
Thin plate spline (TPSn)	$r^n \log(r), n \text{ even}$
Multiquadric (MQ)	$\sqrt{1 + r^2}$

RBF with global support	$\varphi(r)$
Inverse multiquadric (IMQ)	$\frac{1}{\sqrt{1+r^2}}$
Inverse quadratic (IQ)	$\frac{1}{1+r^2}$
Gaussian (GS)	e^{-r^2}
RBF with compact support	$\varphi(r) = f(\xi), \xi \leq 1, \xi = \frac{r}{R_{sup}}$
Wendland (C^0)	$(1-\xi)^2$
Wendland (C^2)	$(1-\xi)^4(4\xi+1)$
Wendland (C^4)	$(1-\xi)^6\left(\frac{35}{3}\xi^2+6\xi+1\right)$

Table 1: Typical Radial Basis Functions

A linear system (of order equal to the number of source point introduced [10]) needs to be solved for coefficients calculation. Operatively, once the RBF system coefficients have been calculated, the displacement of an arbitrary node of the mesh, either inside (interpolation) or outside (extrapolation) the domain, can be expressed as the sum of the radial contribution of each source point (if the point falls inside the influence domain). In such a way, a desired modification of the mesh nodes position (smoothing) can be rapidly applied preserving mesh topology. An interpolation function s composed by a radial basis φ and the aforementioned polynomial h of order $m-1$, where m is said to be the order of φ , is defined as follows if N is the total number of contributing source points.

$$s(\mathbf{x}) = \sum_{i=1}^N \gamma_i \varphi(\|\mathbf{x} - \mathbf{x}_{k_i}\|) + h(\mathbf{x})$$

The degree of the polynomial has to be chosen depending on the kind of RBF adopted. A radial basis fit exists if the coefficients γ and the weight of the polynomial can be found such that the desired function values are obtained at source points and the polynomial terms give zero contributions at source points, that is:

$$s(\mathbf{x}_{k_i}) = \mathbf{g}_i, \quad 1 \leq i \leq C$$

$$\sum_{i=1}^N \gamma_i p(\mathbf{x}_{k_i}) = 0$$

for all polynomials p with a degree less or equal than that of polynomial h . The minimal degree of polynomial h depends on the choice of the RBF. A unique interpolator exists if the basis function is a conditionally positive definite function [10]. If the basis functions are conditionally positive definite of order $m \leq 2$ [12] a linear polynomial can be used:

$$h(\mathbf{x}) = \beta_1 + \beta_2 x + \beta_3 y + \beta_4 z$$

The subsequent exposition assumes that the aforementioned hypothesis is valid. A consequence of using a linear polynomial is that rigid body translations are exactly recovered. The values for the coefficients γ of RBF and the coefficients β of the linear polynomial can be obtained by solving the system:

$$\begin{pmatrix} M & P \\ P^T & 0 \end{pmatrix} \begin{pmatrix} \gamma \\ \beta \end{pmatrix} = \begin{pmatrix} g \\ 0 \end{pmatrix}$$

where g are the known values at the source points. M is the interpolation matrix defined calculating all the radial interactions between source points:

$$M_{ij} = \varphi \left(\left\| \mathbf{x}_{k_i} - \mathbf{x}_{k_j} \right\| \right), 1 \leq i \leq C, 1 \leq j \leq C$$

and P is a constraint matrix that arises imposing the orthogonality conditions and contains a column of “1” and the x y z positions of source points in the others three columns:

$$P = \begin{pmatrix} 1 & x_{k_1} & y_{k_1} & z_{k_1} \\ 1 & x_{k_2} & y_{k_2} & z_{k_2} \\ \vdots & \vdots & \vdots & \vdots \\ 1 & x_{k_N} & y_{k_N} & z_{k_N} \end{pmatrix}$$

Radial basis interpolation works for scalar fields. For the smoothing problem, each component of the displacement field prescribed at the source points is interpolated as follows:

$$\begin{cases} s_x(\mathbf{x}) = \sum_{i=1}^N \gamma_i^x \varphi(\|\mathbf{x} - \mathbf{x}_{k_i}\|) + \beta_1^x + \beta_2^x x + \beta_3^x y + \beta_4^x z \\ s_y(\mathbf{x}) = \sum_{i=1}^N \gamma_i^y \varphi(\|\mathbf{x} - \mathbf{x}_{k_i}\|) + \beta_1^y + \beta_2^y x + \beta_3^y y + \beta_4^y z \\ s_z(\mathbf{x}) = \sum_{i=1}^N \gamma_i^z \varphi(\|\mathbf{x} - \mathbf{x}_{k_i}\|) + \beta_1^z + \beta_2^z x + \beta_3^z y + \beta_4^z z \end{cases}$$

Radial basis method has several advantages that makes it very attractive in the area of mesh smoothing. The key point is that, being a meshless method, only grid points are moved regardless of element connection and it is suitable for parallel implementation. In fact, once the solution is known and shared in the memory of each calculation node of the cluster, each partition has the ability to smooth its nodes without taking care of what happens outside because the smoother is a global point function and the continuity at interfaces is implicitly guaranteed. Furthermore, despite its meshless nature, the method is able to exactly prescribe known deformations onto the surface mesh: this effect is achieved by using all the mesh nodes as RBF centres with prescribed displacements, including the zero field to guarantee that a surface is left untouched by the morphing action.

RBF Morph ACT Extension

ANSYS® Workbench™ is built on a modular architecture that lets the users extend the functionality of such a numerical environment through add-in software components. In particular, the ACT technology supplies internal mechanisms conceived to enable deeply integrated customizations of a Workbench application that can also make use of a connection with the inner libraries. Exploiting that framework, RBF Morph, already well known for the morphing and shape optimization ground-breaking add-on tailored for ANSYS® Fluent®, is also available as an ACT extension for Mechanical [13] with which shares the same look & feel as well as the interaction logic including the scoping tools for geometrical and mesh elements selection.

When the RBF Morph Extension is enabled a custom toolbar gets integrated in the Mechanical interface and an RBF Morph object can be added in the Mechanical tree between the mesh and the solver branch (see Figure 2) in the respect of its function of mesh modifier. To handle complex mesh modifications the morpher tool has a hierarchical working logic that foresees the use of multiple children (also called RBF Sources). Each child in the RBF Morph tree is a shape modifier acting on its selection (nodal, geometrical and named selections are available) and propagating it to its father (this selection is called RBF Target).

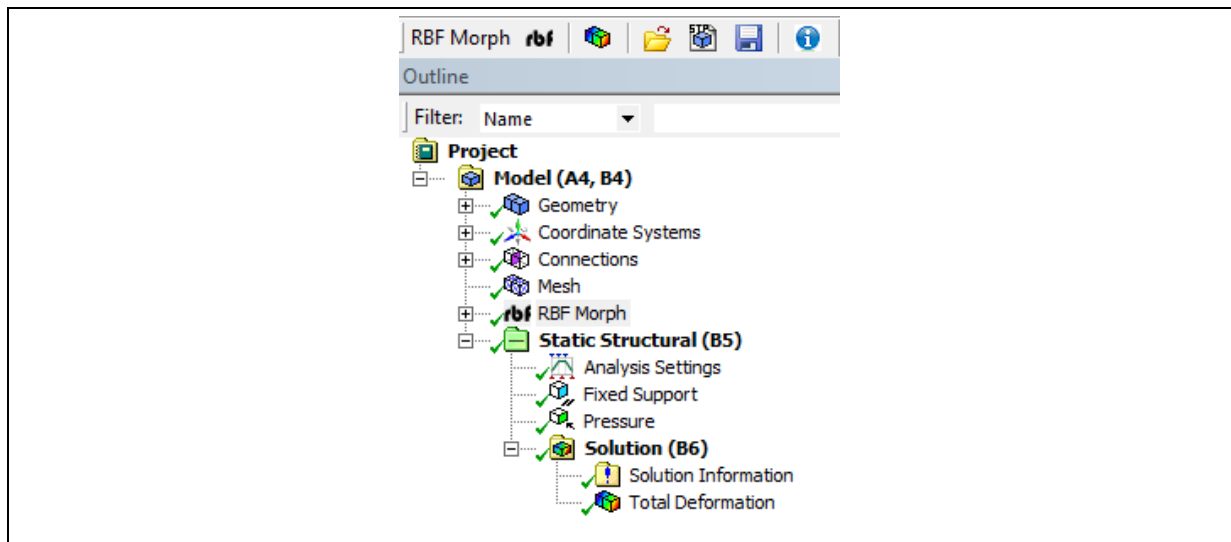


Figure 2: RBF Morph Extension position in the Mechanical tree

Several shape modifications are available including Translation, Rotation, Scaling, Curve and Surface Offset as well as Curve and Surface Targeting. For Translation, Scaling and Rotation a custom coordinate systems to shorten the morphing setup can be selected. Other available options are the order of the RBF used (linear or cubic) and the feature to apply the shape modification to the baseline mesh or to the already modified grid.

For each RBF Source the resulting behaviour can be interactively previewed for checking and, once the set-up is completed, the mesh can be morphed either in serial manner or exploiting CUDA or OpenMP acceleration. The modified shape can be analysed by applying morphing and interacting with the post-processing tools of Mechanical manually, or by using parameters so that the automation and the optimization tools supplied by Workbench can be exploited at best. Once the optimal geometry is identified, the optimal CAD can be finally generated by means of the back to CAD feature morphing the baseline NURBS geometry or by exploiting the FEModeler back to CAD capabilities.

Figure 3 illustrates the most general Workbench project dealing with RBF Morph Extension based optimization.

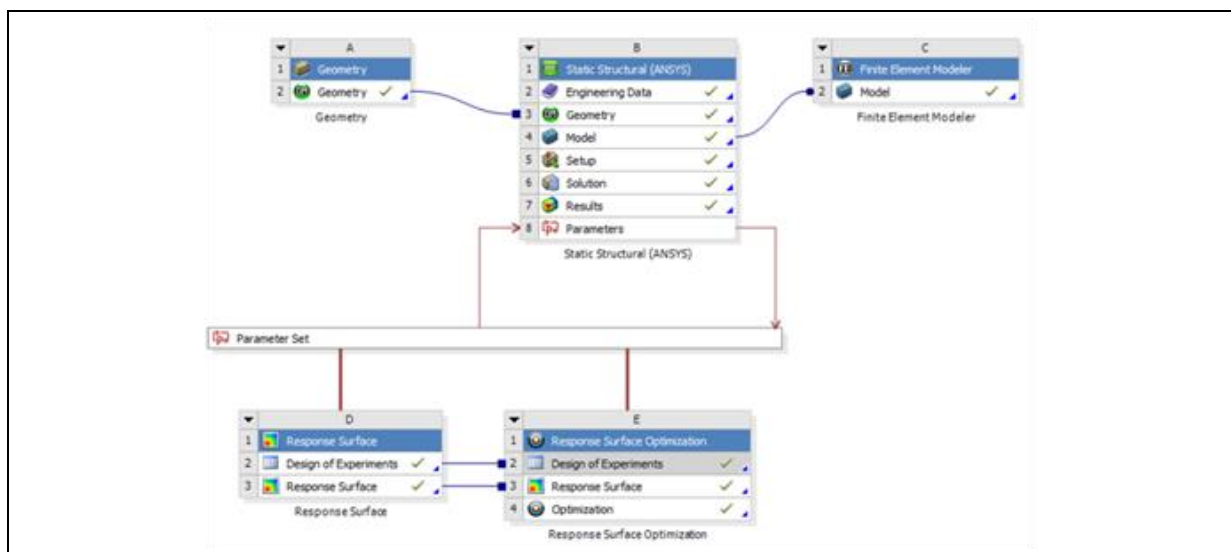


Figure 3: Workbench project concerning RBF Morph Extension

The process begins with the import or the modelling of the components to be studied. Successively the system is analysed and, taking into account the results, the shape modifications are suitably designed and parameterized to search for the optimal shape through an optimization process characterized by a high level of automation. Once the optimal geometry is gained, its CAD representation can be finally generated.

Application description

The optimization study of the automotive wheel rim has the objective to reduce the weight of such a component guaranteeing at the same time its structural integrity. The starting (baseline) geometry of the wheel rim, whose CAD model is visualized in Figure 4 from a frontal view, has a total mass of 7.526 kg and, with regard to the shape modifications to be applied, the intervention area is restricted to the spokes set, whose cross section is specifically intended to be shrunk to lighten the structure with a controlled increase of the stress level.



Figure 4: CAD model of the automotive wheel rim of the study in the baseline configuration

Specifically referring to the main characteristics of the component, it is made of aluminium casting alloy (AlSi7Mg), it has an external radius of 0.22m, and it shows a pattern consisting of 8 identical spokes aligned along the radius with 8 connecting holes equally spaced along the circumference. The properties' values of the material are collected in the following table

Property	E (MPa)	ν (-)	S_y (MPa)	S_u (MPa)	S_F (MPa)	ρ (kg m ⁻³)
Value	$71 \cdot 10^3$	0.33	280	314	89	2770

Table 2: Material's properties

where E is the Young's Modulus, ν is the Poisson's ratio, S_y , S_u and S_F respectively are the tensile yield strength, the tensile ultimate strength and the fatigue strength. For design purposes, loads have been applied in the respect of the TÜV standard [14] which prescribes a series of tests that an automotive wheel rim has to stand to be homologated. In particular, the following three main loading scenarios shall be taken into account:

1. Alternating bending moment (ABM): it mimics the alternating bending moment test that basically pertains to the load that acts on the wheel while steering. Two specific load conditions are required to be considered:

- a. 50% of the maximum bending moment for $1.8 \cdot 10^6$ cycles;
 - b. 75% of the maximum bending moment for $2 \cdot 10^5$ cycles.
2. Alternating torque (AT): it reproduces the alternating torque test and appertains to the load that acts on the wheel while braking / accelerating. Such a test requires the wheel to sustain the maximum torque for 10^6 cycles;
 3. Car weight (CW): it mimics the car weight test that deals with the car weight acting on the wheel while driving on a straight way. Such a test is judged fulfilled if the wheel stands the total vertical force for $1.33 \cdot 10^6$ cycles.

The maximum bending moment M_{bm} , the maximum torque M_t and the maximum vertical force F_w are respectively given by the following relationships:

$$M_{bm} = f_{bm} \cdot F_R \cdot (\mu \cdot r + e)$$

$$M_t = f_t \cdot F_R \cdot r$$

$$F_w = f_w \cdot F_R$$

where F_r is the static load acting on a wheel, f_{bm} is the bending moment safety factor, f_t is the torque safety factor f_w is the car weight safety factor, μ is the friction coefficient, r is the tire outer radius and e is the wheel (positive) offset. The values of the just listed parameters to be employed for running FEM verification analyses are specified in Table 3.

Parameter	F_R (kg)	f_{bm} (-)	f_t (-)	f_w (-)	μ (-)	r (m)	e (m)
Value	650	2	1	2.5	0.9	0.940	0.014

Table 3: Values of the parameters used to determine loading scenarios

To effectively identify a threshold level over which the component integrity is not guaranteed, a Failure Index (FI) has been defined for each load scenario according to a fatigue failure condition. In specific, FI is defined as the ratio between the calculated maximum structural stress and the material allowable strength, namely

$$FI = \frac{\sigma_{MAX}}{\sigma_{allowable}}$$

where the material allowable strength can be determined as [15]

$$\sigma_{allowable} = \frac{1}{\gamma_k} \cdot \frac{\sigma_{D-1} \cdot \kappa_k \cdot \kappa_n \cdot \kappa_t}{\kappa_f \cdot \kappa_d \cdot \kappa_i \cdot \kappa_c}$$

where σ_{D-1} is the fatigue strength of the material, κ_k is the cycle pattern factor, κ_n is the equivalent number of cycles factor (Table 4), κ_t is the loading factor, κ_f is the stress concentration factor, κ_d is the size factor, κ_i is the surface factor, κ_c is the corrosion factor and γ_k is the fatigue safety factor, and in the case FI is higher than unity the structural trustworthiness is evaluated as jeopardized. The values of the factors employed for material allowable stress calculation are gathered in Table 5.

	ABM 50%	ABM 75%	AT	CW
κ_n	1.48	1.84	1.57	1.53

Table 4: Fatigue factors κ_n used for allowable stress calculation for the different TÜV tests

Fatigue factor	κ_k	κ_f	κ_t	κ_d	κ_i	κ_c	γ_k
Value	1	1	1	1	1.25	1	1.12

Table 5: Values of fatigue factors used for allowable stress calculation

Adopting the values and the procedure above described, the material allowable threshold stress levels to be used in FEM verification have been calculated. Such values are summarized in Table 6.

TÜV test	ABM 50%	ABM 75%	AT	CW
$\sigma_{\text{allowable}}$ (MPa)	94	116	100	97

Table 6: Value of the material allowable thresholds

In the next paragraph the description of the numerical strategy adopted to carry out the optimization study is detailed.

Adopted numerical strategy

The numerical strategy employed to accomplish the optimization study, foresees two main phases to be performed in sequence. In the first one, the baseline geometry of the wheel rim is analysed to verify whether the structure passes the TÜV standard tests, that is if all FIs are below unity, whilst in the second stage the morphing action on the spokes is designed and successively applied in manual fashion till the maximum FI reaches a value just lower than unity.

The manual operation has been performed in the respect of the scope of the second stage of the explorative set of analyses concerning the RBF Morph ACT Extension. These analyses have been scheduled to have an incremental level of complexity and sought automation. As a matter of fact, in the first phase of the numerical investigation the morphing of a single spoke has just been taken into account, whilst in the third one the FEM computing will be automated using parameters including all spokes with several shape modifications.

Baseline configuration analysis set-up

Overall analysis set-up

As not all loads to be set have a cyclic symmetry characteristic, the entire component needs to be accounted in FEM simulations. Given that, after the CAD model available in Parasolid format has been imported in ANSYS® DesignModeler™, the mesh has been generated through ANSYS® Meshing™ adopting the advanced size function on curvature. The final discretization is approximately composed by $193 \cdot 10^3$ quadratic tetrahedrons (SOLID187) and $327 \cdot 10^3$ nodes. A detail of the surface mesh is depicted in Figure 5.

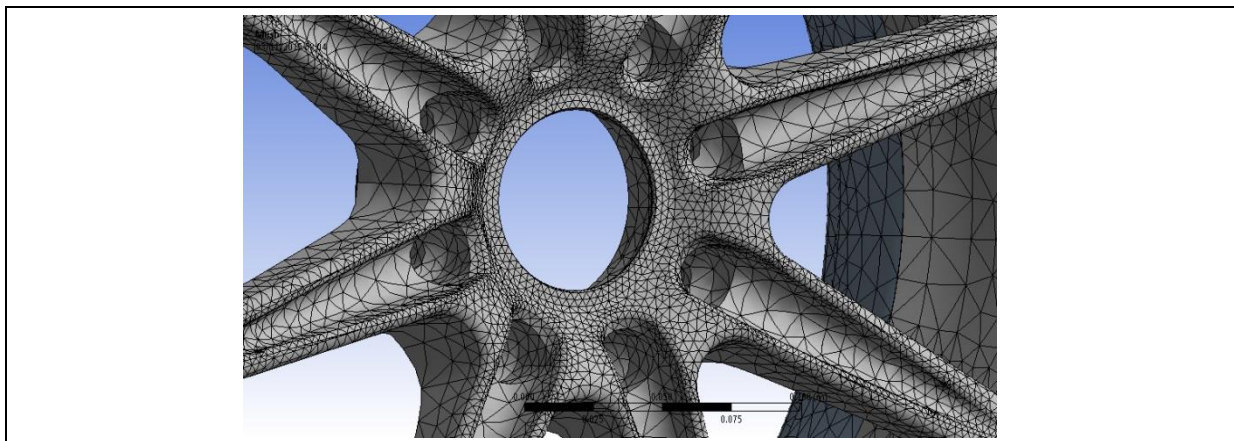


Figure 5: Mesh detail

The performed simulations assumed that the material is isotropic and behaves as linear. Moreover, neither thermal contribution has been accounted nor pre-stressed field has been assigned.

To ease the management of all the loading scenarios in the same environment both before and after morphing, a Workbench project has been built up including five cells of static analysis. In specific, the first two cells pertain to the alternating bending moment, the third one to the alternating torque, the fourth one to the car weight, whilst the last one has been created to monitor the mass of the entire component after computing through an APDL routine.

Referring to computational outputs, the maximum deformation and maximum equivalent von Mises stress have been set for each static analysis, and this latter result has been also utilized as maximum stress in a further user defined result to determine the FI.

Loading scenarios detail

Relating to alternating bending moment, 50% and 75% of the maximum bending moment, respectively equal to 1100 N·m and 1650 N·m, have been applied to the internal surfaces of the connecting holes and the main hole by means of the Remote Point feature of the FEM solver. Finally what is visualized in Figure 6a has been got. With regard to constraints, the external surfaces in contact to the tire, and highlighted in Figure 6b, have been maintained fixed by means of a fixed support. Such a constraint together with the loaded surfaces are the settings present in all loading scenarios.

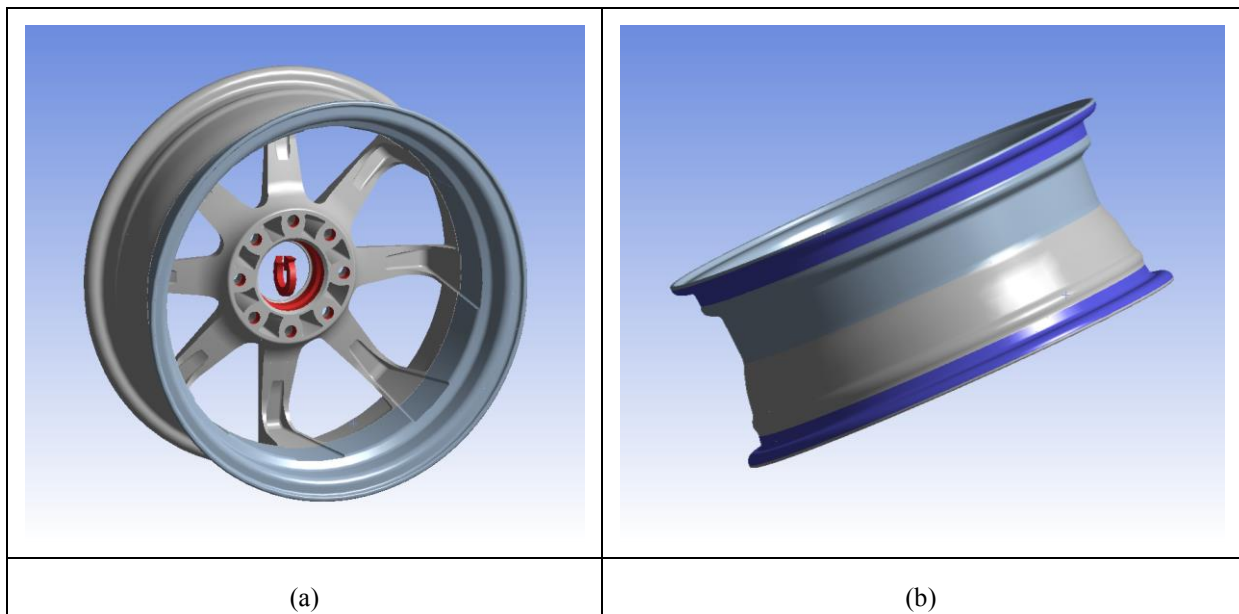


Figure 6: Alternating bending moment and fixed support application

Referring to alternating torque, a value of 1530 N m has been assigned as depicted in Figure 7a, whilst load dealing with the car weight scenario has a value of 15940 N and it has been set to obtain what depicted in Figure 7b.

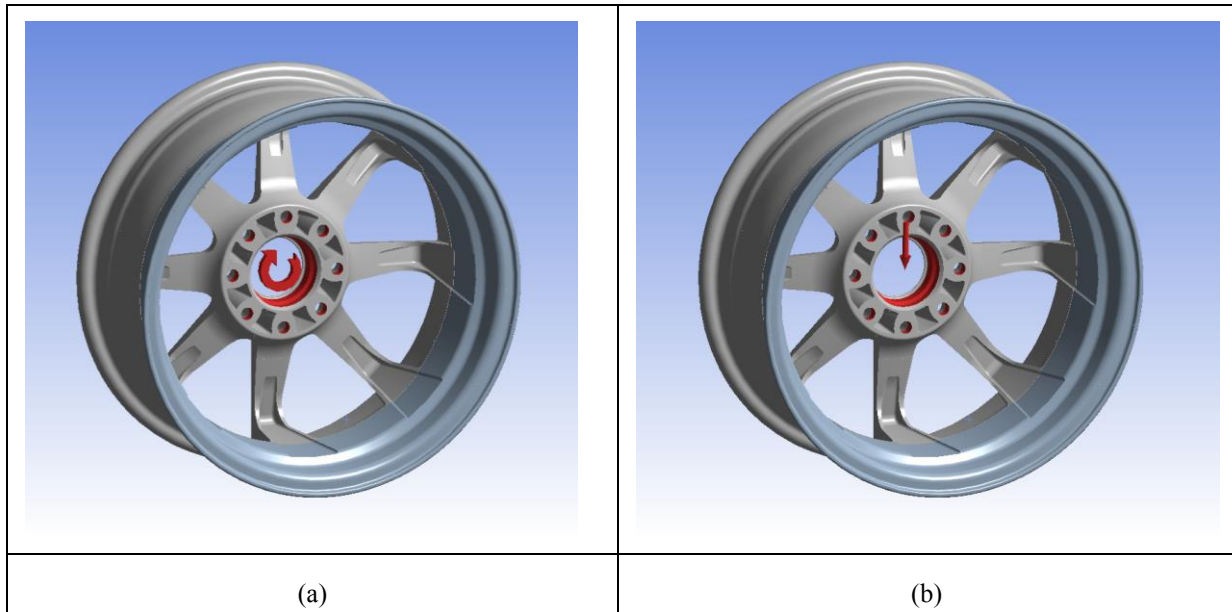


Figure 7: Alternating torque and car weight application

The results automatically gained in sequence after running the Workbench project concerning the baseline configuration are summarized in the following paragraph.

Baseline configuration analysis results

For the alternating bending moment load scenario, Figure 8 shows the equivalent von Mises stress distribution for the 50% and 75% case, on the left and right side respectively and according to a deformed visualization in auto-scale mode.

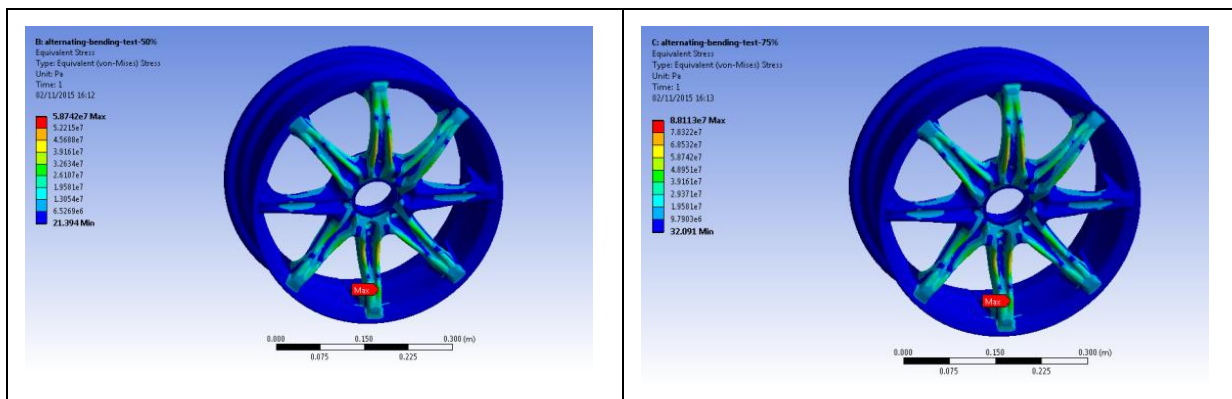


Figure 8: Equivalent stress for the alternating bending moment loads

Following the same type of visualization, Figure 9a and Figure 9b respectively depict the data obtained for the alternating torque and car weight loading scenario.

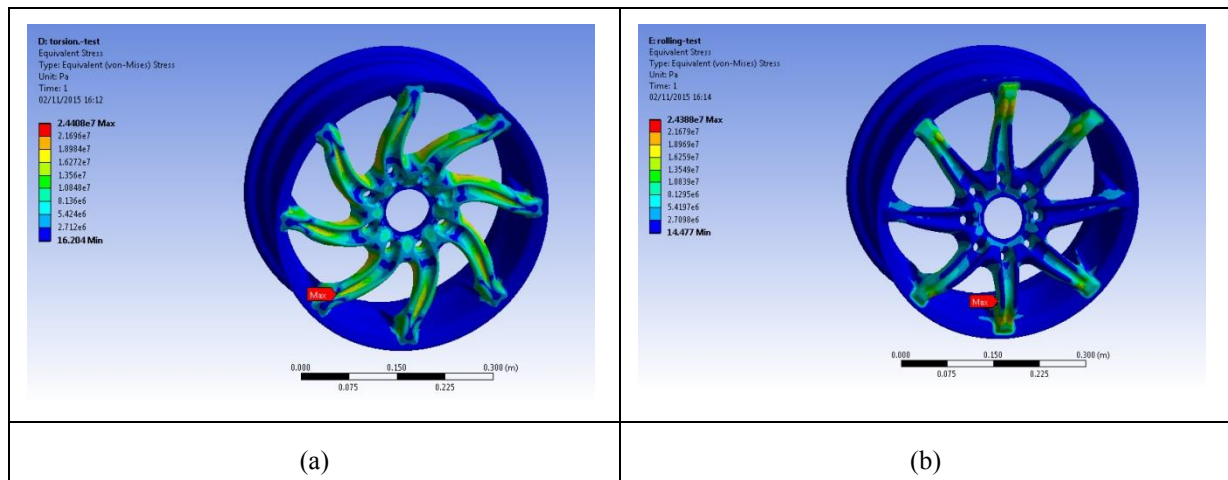


Figure 9: Equivalent stress for the alternating torque and car weight load

The FIs calculated at the end of the baseline analysis are listed in Table 7. Such a data defines the main result of the first stage of the whole optimization analysis.

TÜV test	ABM 50%	ABM 75%	AT	CW
FI	0.62	0.76	0.24	0.25

Table 7: Static analysis FIs of the baseline geometry

As it can be judged, the component does not fail as all resulting FIs are minor than 1 and a particular attention must be paid to the 75% bending moment test after the shape modifications are applied through morphing because this load has the highest value of the FI.

Morphing

The morphing set-up consists of one single RBF Target and ten first level RBF Sources as depicted in Figure 10. Specifically the entire wheel rim model has been assigned as Target, while Sources have been created to morph the eight spokes and to maintain unchanged the position of the nodes of internal holes (connecting holes and main hole) surfaces and the surfaces in contact to the tire. To facilitate the accomplishment of the morphing setting up of Sources, suitable named selection worksheets to pick up the nodes involved in the morphing action had been properly defined in advance.

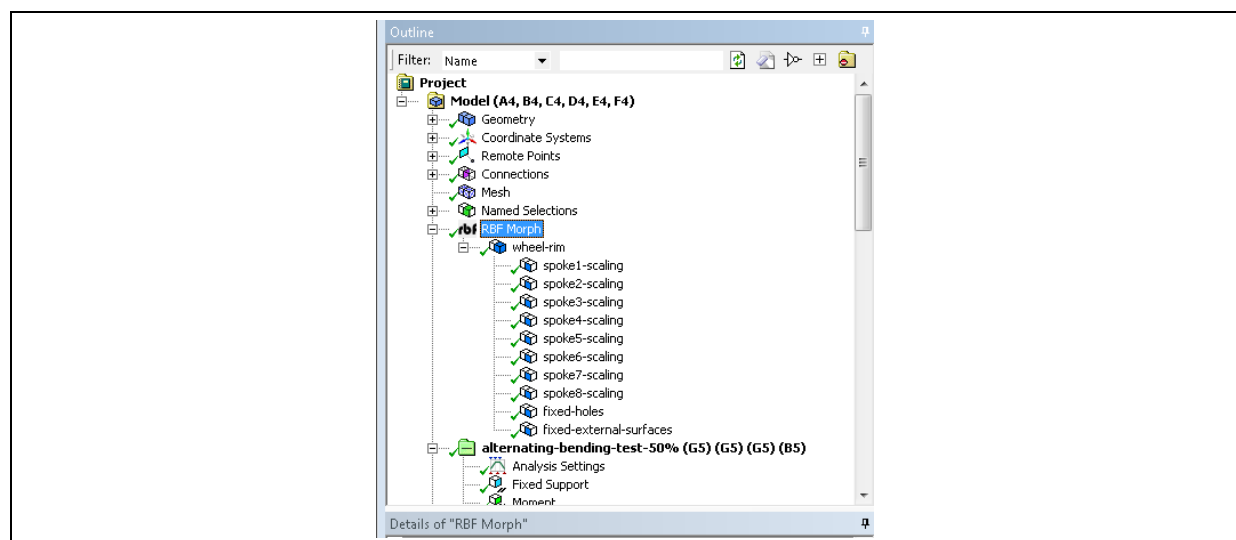


Figure 10: RBF Morph tree for the morphing set-up

The scaling feature of the morpher tool has been utilized to shrink each spoke with respect to the y axis of a custom coordinate system having the origin in the plane of symmetry of its largest faces. As such, just a single parameter drives the shape modification of each spoke. To ease the comprehension of the local effect of morphing, Figure 11 shows the preview of source nodes of one of the generated Sources in the case of y component of scaling equal to 0.8. In specific, the preview is a useful feature that permits to visualize the location of source nodes before (red points) and after (blue points) the application of morphing without effectively executing the mesh smoothing.

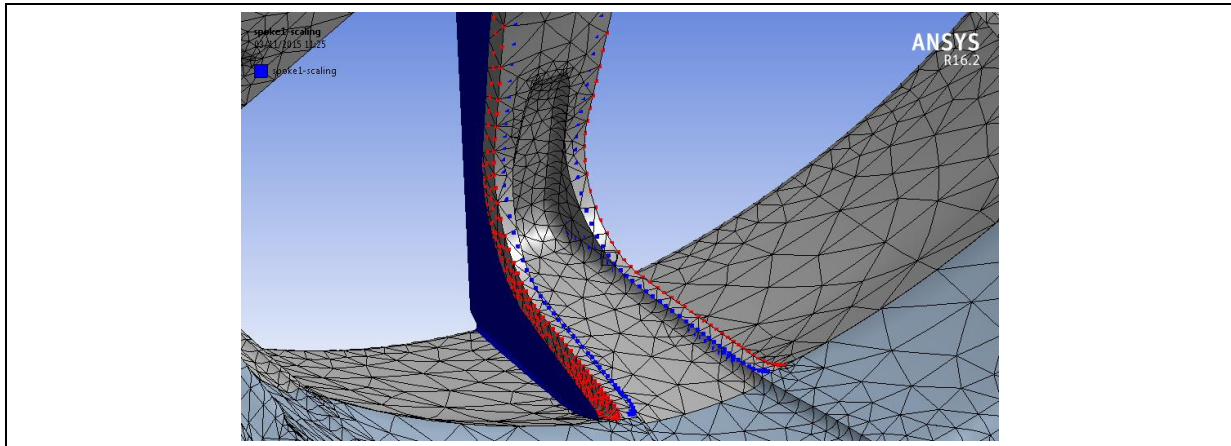


Figure 11: Source nodes preview of the Source dealing with a spoke

The latter two Sources are aimed at defining the fixed boundaries, namely the nodes onto the morphing domain interface that are required to remain fixed during the morphing action. The preview of such sources is depicted in Figure 12a and Figure 12b that respectively concern the internal connecting holes and external surfaces. The whole morphing configuration has required 10-15 minutes to be set by a medium skilled user.

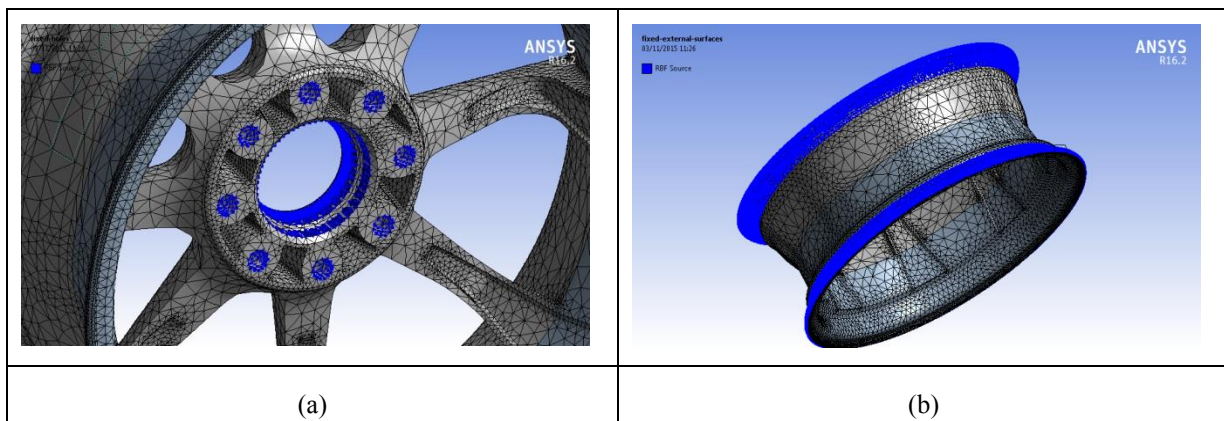


Figure 12: Source nodes preview the sources dealing with fixed surfaces

The main results of optimization are reported in the following paragraph.

Results of optimization

The morphing plan envisages to reduce the cross section of the spokes with the limit of 1 for the highest FI. Since it has been decided to perform the shape optimization manually, for each modification of the wheel rim a Workbench project update needs to be sequentially accomplished to evaluate the resulting FIs. To pass from one to another modification, the undo feature of the morpher

tool shall be used. Given that, 0.8 and 0.7 are the first values imposed for the scaling factor in view of running in sequence FEM analyses.

Since for the 0.7 case the FI related to 75% alternating bending moment load is higher than 1, 0.72 has been finally tried. This value has allowed to get a maximum FI of 0.99 that has been judged satisfying taking into account the scope of the optimization. The FIs of the morphed configurations gained throughout the optimization stage are collected in Table 8.

TÜV test	ABM 50%	ABM 75%	AT	CW
FI scaling 0.8	0.75	0.91	0.33	0.31
FI scaling 0.7	0.83	1.19	0.41	0.39
FI scaling 0.72	0.82	0.99	0.39	0.34

Table 8: Static analysis FIs of the optimization stage

Figure 13 illustrates a comparison between the equivalent stress of the baseline (Figure 13a) and the optimal shape (Figure 13b) of the wheel rim.

As expected, the highest value of the FI resulted from the 75% bending moment test and the final configuration of the wheel is lighter than the previous, without the risk of failure. Taking this load scenario as reference, the optimization process has led to a configuration with an increase of the FI and maximum stress respectively of 25% and 23%, whilst the achieved mass reduction is almost 0.5 kg equal to a -6.6% improvement with respect to the baseline configuration.

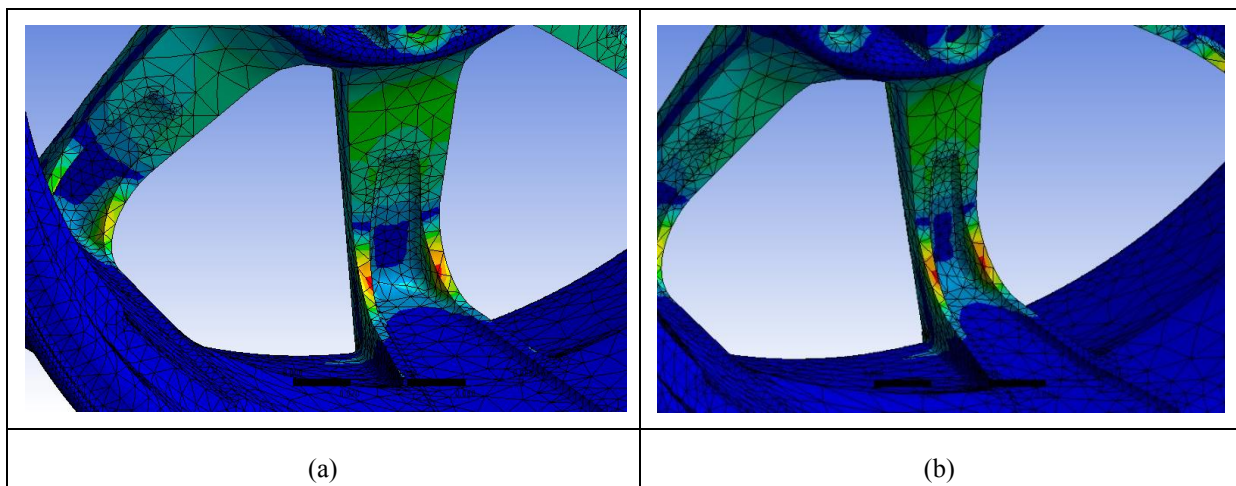


Figure 13: Comparison between the baseline and the optimal component stress field

To close the optimization process the obtained geometry has been finally exported back to CAD using FE Modeler. The generated geometry, opened in DesignModeler, is shown in Figure 14.

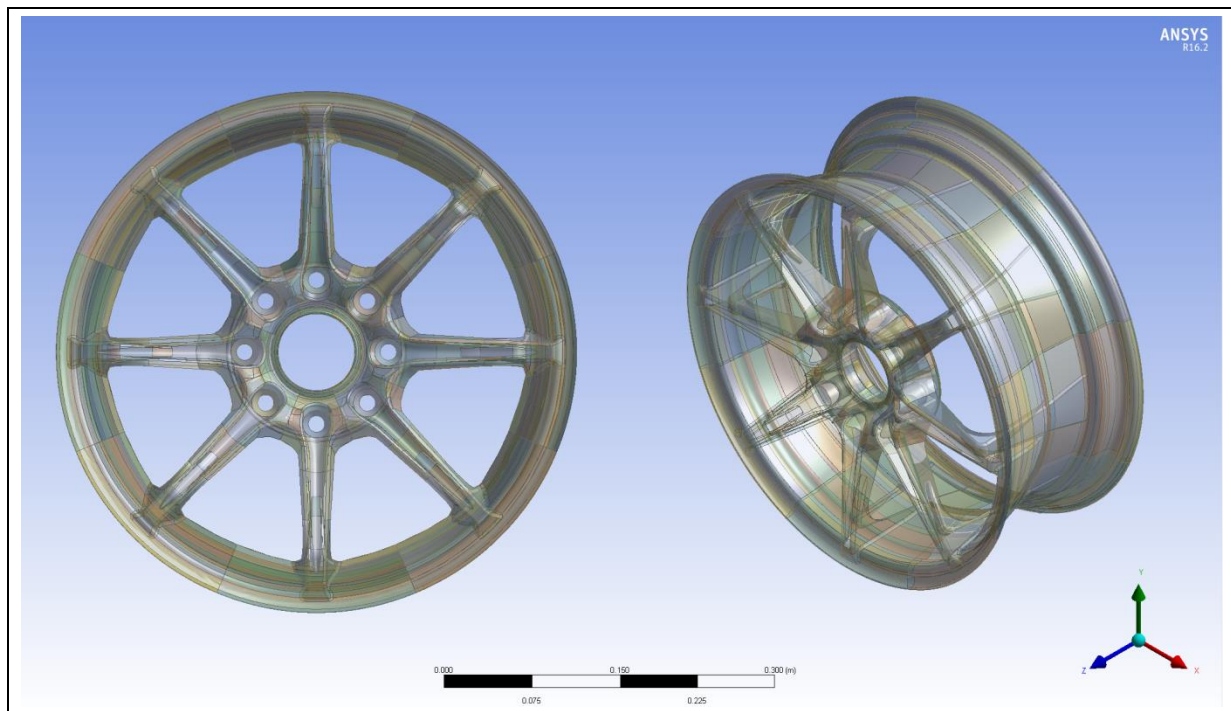


Figure 14: Optimized geometry obtained by means of the back to CAD feature

Since the CAD model has been imported because already generated by a third party company, a comparison with a CAD-based optimization in terms of the time needed to perform a parametric study has not been feasible. Considering that, it is worth underlining the mesh morphing based approach has effectively enabled the optimization study also in this quite common industrial practice even when a FEA team works in collaboration with other teams of the same firm.

Conclusions

Advanced radial basis functions morphing of RBF Morph has been used to re-shape an automotive wheel rim in order to reduce its weight preventing at the same time the structural failure of the component. The environment chosen to perform the study has been ANSYS Workbench with integrated the RBF Morph ACT Extension. Loads scenarios have been set according to the TÜV standard prescribing how to apply boundary conditions on a wheel rim in a series of tests in order to be homologated. First of all, a structural analysis of the baseline configuration has been run to assess the starting point in terms of stresses acting on the component and, consequently, possibilities of improvement. Being the loads not symmetrical, the entire geometry has been studied. Preliminary analyses have showed that the structure was not exploited to its maximum considering that a reserve of fatigue life was left and a weight lightening would have been possible. The cross sections of the wheel rim spokes have been progressively reduced by means of morphing tool action, with a decreasing scaling factor and monitoring the resulting FI values. The shrinkage of the spokes has been stopped when the value of the highest FI reached 0.99. This last is the chosen optimal configuration for the wheel rim, i.e. the lightest possible before fatigue failure, with a 6.6% weight reduction on an already optimised geometry. The integration of RBF Morph technology in ANSYS Mechanical has proven to provide the user with the possibility to manage complex models and perform shape optimization studies directly inside a familiar and efficient working environment in short time.

References

- [1] M. P. Bendsoe, O. Sigmund.: “Topology Optimization, Theory Methods and applications”, Springer Verlag, 1-47 (2003)
- [2] A. Falk, F.J. Barthold, E. Stein.: “A hierarchical design concept for shape optimization based on the interaction of CAGD and FEM”, Structural Optimization, 18, 12-23 (1999)
- [3] Y. Ding.: “Shape optimization of structures: a literature survey”, Computers & Structures, 24:6, 985-1004, (1986)
- [4] A. Schleupen, K. Maute, E. Ramm.: “Adaptive FE-procedures in shape optimization”, Structural and Multidisciplinary Optimization, 19, 282-302, (2000)
- [5] G. Augugliaro, M. E. Biancolini.: “Optimisation of fatigue performance of a titanium connecting rod”, SAE technical paper 980800, 1-3 (2003)
- [6] D. Sieger, S. Menzel, M. Botsch, “RBF morphing techniques for simulation-based design optimization”, Engineering with Computers, 30, 2, 161-174 (2014)
- [7] M.E. Biancolini.: “Mesh Morphing and Smoothing by Means of Radial Basis Functions (RBF): A Practical Example Using Fluent and RBF Morph”, Handbook of Research on Computational Science and Engineering: Theory and Practice, IGI Global, ISBN13: 9781613501160, (2011)
- [8] P. J. Davis.: “Interpolation and approximation”, Blaisdell, London 1963
- [9] A. De Boer, M.S. Van der Schoot, H. Bijl.: “Mesh deformation based on radial basis function interpolation”, Computers and Structures, Vol. 85, Nos. 11-14, 2007, pp. 784-795
- [10] M.D. Buhmann.: “Radial Basis Functions”, Cambridge University Press, New York (2003)
- [11] C. Micchelli.: “Interpolation of scattered data: Distance matrices and conditionally positive definite functions”, Constructive Approximation, Vol. 2, No. 1, pp. 11-22 (1986)
- [12] A. Beckert, H. Wendland.: “Multivariate interpolation for fluid-structure-interaction problems using radial basis functions”, Aerospace Science and Technology, Vol. 5, No. 2, pp. 125-134 (2011)
- [13] R. Cenni, C. Groth, M.E. Biancolini.: “Structural optimisation using advanced Radial Basis Functions mesh morphing”, AIAS 2015 – 503 (2015)
- [14] TÜV Rheinland@.: “Type Testing for Wheels and Tires”. Retrieved May 2007 from http://www.tuv.com/en/corporate/business_customers/vehicles_traffic_2/development_type_testing_1/wheels_tires_1/wheels_tires.html (accessed on 11th November 2015)
- [15] C. Brutti.: “Introduzione alla progettazione meccanica”, Levrotto & Bella (2002)

Definitions, Acronyms and Abbreviations

ABM	Alternating Bending Moment
ACT	Application Customization Toolkit
APDL	ANSYS Parametric Design Language
AT	Alternating Torque
CAD	Computer Aided Design
CW	Car Weight
CUDA	Compute Unified Device Architecture

FEA	Finite Element Analysis
FEM	Finite Element Method
FI	Failure Index
NURBS	Non-Uniform Rational Basis Spline
OpenMP	Open Multiprocessing
RBF	Radial Basis Functions